Original Research Article

The Egyptian Journal of Immunology

The Egyptian Journal of Immunology,
E-ISSN (2090-2506)
Volume 31 (3), July, 2024
Pages: 95–112.
www.Ejimmunology.org
https://doi.org/10.55133/eji.310310

Immunogenicity study of a Novel DNA-Based HCV vaccine candidate

Eman A. Salem[1], Ashraf Tabll[1, 2], Tamer Z. Salem[3], Yasmine S. El-Abd[1], Reem El-Shenawy[1], Heba Shawky[4], and Sahar Shoman[5]

[1]Department of Microbial Biotechnology, Biotechnology Research Institute, National Research Centre, Cairo, Egypt.

[2]Egypt Center for Research and Regenerative Medicine (ECRRM), Cairo, Egypt.

[3]Molecular Biology & Virology Lab, Center for X-Ray Determination of the Structure of Matter (CXDS), Zewail City of Science & Technology, Giza, Egypt.

[4]Department of Therapeutic Chemistry, Pharmaceutical & Drug Research Institute, National Research Centre, Cairo, Egypt.

[5]Department of Microbiology, Faculty of Science, Ain Shams University, Cairo, Egypt.

Corresponding author: Yasmine S. El Abd, Department of Microbial Biotechnology, Biotechnology Research Institute, National Research Centre, Cairo, Egypt.
Email: yasminco@yahoo.com

Abstract

In this study, we aimed to evaluate the immunogenic profile of a chimeric DNA-based hepatitis C virus (HCV) vaccine candidate encoding the full-length viral core–E1–E2 (HCV-CE) fragment. The vaccine candidate was designed to uniformly express the HCV genotype 4 core-E1-E2 protein. The recombinant HCV-CE protein was bacterially expressed in C41 (DE3) cells, and then BALB/c mice were immunized with different combinations of DNA/DNA or DNA/protein prime/boost immunizations. The proper construction of our vaccine candidate was confirmed by specific amplification of the encoded fragments and basic local alignment search tool (BLAST) results of the nucleotide sequence, which revealed a high degree of similarity with several HCV serotypes/genotypes. The platform for bacterial expression was optimized to maximize the yield of the purified recombinant HCV-CE protein. The recombinant protein showed high specific antigenicity against the sera of HCV-infected patients according to the ELISA and western blot results. The predicted B- and T-cell epitopes showed high antigenic and interferon-γ (IFN-γ) induction potential, in addition to cross-genotype conservation and population coverage. The mice antisera further demonstrated a remarkable ability to capture 100% of the native viral antigens circulating in the sera of HCV patients, with no cross-reactivity detected in control sera. In conclusion, the proposed HCV vaccination strategy demonstrated promising potential regarding its safety, immunogenicity, and population coverage.

Keywords: HCV; Core; E1/E2; Prophylactic vaccination; DNA vaccine; Immuno-informatics; Immune response.

Date received: 15 October 2023; **accepted:** 29 May 2024

Introduction

Although the hepatitis C virus (HCV) elimination strategy adopted by the World Health Organization (WHO) targets an 80% reduction in the incidence of HCV by 2030, few countries are on-target to achieve such a reduction goal. According to the most recent WHO report in 2024, the number of new HCV infections is estimated to be 1.5–2 million/year worldwide,

despite the advent of effective direct-acting antivirals (DAAs).[1] Indeed, the introduction of DAAs has extraordinarily increased the cure rate worldwide. However, a minimal margin (<7%) of resistance was recently reported in clinical trials, while higher rates were reported in real-life treatment programs as a result of lower treatment compliance, particularly among hard-to-treat populations.[2,3] The main concern associated with such failure rates, despite being rare, is the emergence of multidrug-resistant variants that jeopardize overall treatment success upon transmission.[4] It should also be noted that successful viral clearance does not guarantee the prevention of re-infection, especially in high-risk individuals, including those receiving drugs, homosexual individuals, and healthcare providers who are frequently prone to blood and/or body fluids.[5-7] These facts render prophylactic HCV vaccine approaches crucial for successful worldwide HCV elimination.

The development of an effective vaccine is largely limited by the extreme heterogeneity of the viral genome that enables immune escape, and host immune pressure induces the generation of genetically distinct viral variants known as "quasispecies", which further contribute to viral immune evasion.[8] HCV structural genes (core and envelope) encode key proteins orchestrating immune-evasive viral activities, among other roles in infection onset and progression. Specifically, the core (nucleocapsid) significantly contributes to infection chronicity by inhibiting cell apoptosis[9] and further activating androgen receptor-mediated transcription that plays a key role in the development of hepatocellular carcinoma in HCV-infected patients.[10] Moreover, the core protein is reported to occlude the initiation of antigen-specific B- and T-cell-mediated immune responses and therefore intercepts specific antiviral responses.[11] On the other hand, the HCV envelope protein (E1-E2) domain, particularly the E2 protein, is the major determinant of infection establishment, where it mediates host cell recognition, entry, and viral assembly.[12] In addition, E2 is a key player in most viral immune evasion strategies at both the humoral and cellular levels, where it reportedly deactivate interferon (IFN)-inducible protein kinase (PKR) crucial for innate antiviral defense mechanisms.[13] Moreover, it mediates the viral evasion of neutralizing antibodies (NAbs) through the hypervariable region 1 (HVR1), which acts as a “decoy epitope” and therefore diverts the humoral response away from conserved epitopes[14]. Furthermore, E2 is known to promote $CD8^+$ T-lymphocyte exhaustion and dysfunction.[15] Nevertheless, it has been reported that protective anti-HCV NAbs are largely directed against epitopes expressed on HCV E1-E2, which might trigger the cellular responses necessary for viral clearance.[16,17] For these reasons, the HCV envelope domain has been an attractive candidate for various HCV vaccines with variable efficacy and delivery strategies, employing different forms of the immunogen, including recombinant, truncated soluble peptides, and adenovirus-based systems.[18-20] However, while the majority of these trials failed to achieve sterilizing immunity[21], it is postulated that early induction of NAbs and cellular responses would contribute to reducing the primary viremic load during acute infection, which may ultimately lower the risk of viral persistence.[22,23] DNA vaccines can effectively mimic the immune dynamics reported during the spontaneous clearance of acute HCV infection, generating consistently upregulated magnitudes of $CD4^+$/$CD8^+$ T cell responses in mice and non-human primates.[24] While DNA-based systems are inherently poor immunogens, it was recently reported that boosting with a secreted form of recombinant E1-E2 proteins, rather than DNA or virus-like particle (VLP)-expressing E1/E2 proteins, significantly increased the immunogenicity of the DNA prime-boost regimen.[25]

The main objective of this study was to design and evaluate the immunogenic profile of a chimeric DNA-based vaccine candidate encoding full-length HCV core–E1–E2 (HCV-CE) fragments both *in-silico* and *in vivo.* The study approach included the assessment of the consensus notion about full-length protein-based HCV vaccines regarding their safety, immunogenicity, and coverage of targeted populations.

Materials and Methods

Designing the HCV-CE construct

A codon-optimized DNA fragment (Addgene, Watertown, Massachusetts; USA) encoding the full-length HCV core-E1-E2 region (GenBank accession number Y11604.1), which was cloned in the pDrive vector (Qiagen; Hilden, Germany). The plasmid construction was confirmed by polymerase chain reaction (PCR) using specific primers for the core, E1, and E2 fragments (Table 1). Each reaction mixture included 50 ng of HCV-CE plasmid used as a template, 10 µl of 10X PCR Buffer, 1 mM dNTPs (QIAGEN; Hilden, Germany), each primer at a final concentration of 200 nM, 5 U of Hotstart Phusion Polymerase (QIAGEN; Hilden, Germany), and 1 µl of DMSO, and the reaction volume was adjusted to 50 µl with nuclease-free H_2O.The cycling conditions were as follows: a single pre-denaturing cycle at 98°C for 30 sec; 35 cycles each of denaturing at 98°C for 10 sec, annealing at 62-65°C, and extension at 72°C for 30 sec-1 min; and a final extension cycle at 72°C for 10 min. The PCR products were visualized in 1% agarose mixed with 0.3% ethidium bromide.

Table 1. Specific primers used for confirmatory PCR amplification.

	Primer ID	Primer sequence	Reference
1.	Core F:	5'-AGCACGAATCCTAAACCTCAAAGAAAAACC-3'	MZ322083.1
2.	Core R:	5'-GGGACAGTCAGGCACGAAAG-3'	
3.	E1 F:	5'-CACTGGACCACCCAGGATTGCA-3'	[39]
4.	E1 R:	5'-GCATCAACCCCTGCAAAGA-3'	
5.	E2 F:	5'- CACTGGGGTGTCCTCGTGGG-3'	
6.	E2 R:	5'-TGGATGAACAGTACCGGGTTCA-3'	

Construction of a DNA vaccine and bacterial expression system

The HCV-CE clone was double-digested with different sets of restriction enzymes depending on the target expression vector. For subsequent cloning into the mammalian expression vector, the enhanced green fluorescent protein (EGFP), pEGFP-N1 (Clonetech Biotechnology, USA), both plasmids were digested with the restriction enzymes BamHI and XhoI (New England Biolabs-NEB, Ipswich, MA, USA). For construction of the bacterial expression vector, the HCV-CE fragment was digested from the synthetic construct encoding the full-length core-E1/E2 fragment (GenBank accession number DQ988079) cloned in pSC-A (Agilent Technologies, USA) using the FastDigest KpnI and NotI restriction enzymes (Thermo Fisher Scientific, USA) along with the bacterial expression vector pET29a (Invitrogen, USA). The digested HCV-CE fragments and linearized expression vectors were purified using gel purification (MinElute gel extraction kit; Qiagen) according to the user manual and then ligated using T4 DNA Ligase (New England Biolabs Company (NEB), USA) according to the user manual. A volume of 5µl of each ligation mixture was transformed into 50 µl of competent *E. coli* DH5α or C41 (DE3) by the heat-shock method.[26] The transformation mixtures were incubated for 1h at 37°C and 250 rpm, after which 250 µl of each mixture was cultured on 2XYT agar plates supplemented with 50 mM kanamycin (for both the pEGFP-N1 and pET29a clones) and incubated overnight at 37°C. The successful cloning of the full-length HCV-CE fragment in pEGFP-N1/pET29a was confirmed by PCR using the specific core forward and E2 reverse primers with the aforementioned settings.

Nucleotide Sequencing

The nucleotide sequence of the purified plasmids prepared from the positive HCV-CE clones was confirmed by automated DNA sequencing (Geospiza, Germany). The obtained sequence was then analyzed using the basic local alignment search tool (BLAST) algorithm (http://www.ncbi.nlm.nih.gov).

Expression and Characterization of Recombinant HCV-CE Protein

The expression of recombinant HCV-CE protein was carried out after Shawky et al.[37] with minor modifications. Individual C41(DE3) (Sigma–Aldrich, USA) recombinant bacterial colonies were grown to saturation at 30°C in 10 mL of 2xYT culture media supplemented with 50 µg/mL kanamycin. A volume of 100 mL of LB media supplemented with 50 µg/ml kanamycin was inoculated with 1mL of the grown bacterial culture and then incubated at 30°C and 250 rpm until the optical density at 600 nm reached 0.6-1. Protein expression was induced by adding 0.2 mM isopropyl *b*-D-thiogalactoside (IPTG), and the incubation was resumed overnight at 25°C and 200 rpm. The recombinant protein was then purified through nickel chelate affinity chromatography[37] (QIAGEN; Hilden, Germany), and both crude and purified HCV-CE protein preparations were assessed by sodium dodecyl sulfate–polyacrylamide gel electrophoresis (SDS-PAGE) according to Laemmli[38], while their antigenicity was assessed by western blot according to Towbin et al.[39] using sera from HCV-infected patients as a source of the detector antibodies.

Animal Immunization

Immunization Protocol

A total of 40 female 6–8-week-old BALB/c mice (16–18 g) were obtained from the Animal House of the National Research Centre (NRC), Cairo, Egypt. The mice were housed at an ambient temperature of 25°C with a 12 h/12 h darkness photoperiod and fed standard rodent pellets and water. The animals were acclimated for one week before the experiment and then randomly allocated into four weight-matched groups (*n*=10/group) assigned as: the DNA/DNA-immunized group (which received 50 µg/dose of HCV-CE/pEGFP-N1); the DNA/protein-immunized group (which received primary immunization with 50 µg of HCV-CE/pEGFP-N1 followed by booster immunization with 20 µg of recombinant HCV-CE protein); and the sham and control groups that received the same dose (100 µl) of PBS or empty pEGFP-N1 mammalian expression vector, respectively. Mice were subcutaneously immunized on days 0 and 14 using incomplete Freund's adjuvant at a 1:1 volume ratio to immunogens. The experimental period was 28 days.

Blood sampling

Blood samples were collected weekly in heparinized tubes from the mid-vein of the tail, and plasma/sera were collected by centrifugation at 3000×g for 10 min. Peripheral blood mononuclear cells (PBMCs) were isolated from blood samples collected in the 4th week using density gradient centrifugation over Ficoll 400 (Sigma–Aldrich, USA) according to the manufacturer's user manual.

At the end of the experimental period, the animals were anesthetized with an intraperitoneal injection of ketamine (50 mg/kg) and xylazine (10 mg/kg) and sacrificed by cervical dislocation. Animals from each group were dissected, spleens were carefully excised from each animal, weighed, and the spleen index was calculated by dividing the spleen weight (mg)/body weight (gm) ×10^3 after Li et al.[40] Five spleens of each group were maintained in 10% PBS-buffered formalin for subsequent immunohistochemical assessments, while the rest of the samples were flush frozen at -80°C for homogenization.

Assessment of Immune Responses

The levels of antigen-specific immunoglobulins (IgM/IgG) in the sera of the immunized animals were estimated by the standard protocol of indirect enzyme linked immunosorbent assay (ELISA) according to Engvall and Perlman[41] using recombinant HCV-CE protein as the coating antigen (500 ng/well) and 1/100 diluted mouse serum. The antibody titer was expressed as the fold change (antibody titer in immunized animal/antibody titer in the control) after Shawky et al.[37] For cellular immunity assessments, circulating PBMCs and splenic $CD4^+/CD8^+$ lymphocytes were quantified by commercially available ELISA kits (Cat Nos.SL0716Mo and SL0717Mo; SunLong Biotech, China) according to the manufacturer's instructions. The levels of circulating tumor necrosis factor-α (TNF-α), interferon (IFN)-γ, and interleukin (IL)-10 were estimated using the

corresponding ELISA kits (Cat# BMS607-3, # BMS606-2, and # BMS614INST, respectively, Invitrogen, Thermo Fisher Scientific, USA) according to the manufacturer's instructions. The absorbance of the final ELISA products was measured at wavelengths of 450 nm and 630 nm using a microtiter reader (ELISA Plate Reader Statfax Chromate 4300, USA), and the cut-off value was determined according to the minimum detection limit for each kit.

Immunohistochemistry

Immunohistochemistry was performed using an automated machine (Dako Autostainer Model S3400, Dako Cytomation, Inc., CA, USA). Briefly, paraffin-embedded 4µm splenic sections were deparaffinized, rehydrated, and washed with double distilled H_2O. The endogenous peroxidase activity was blocked by incubating the slides in a 0.03% solution of H_2O_2 in PBS (pH 7.6) at room temperature for 10 min, and 10% normal goat serum was used to inhibit the non-specific antibody binding. The slides were incubated with 1:50 dilutions of $CD4^+/CD8^+$ primary antibodies (Thermo Fisher Scientific, USA) for 12 h at 4°C. After being rinsed with Tris-buffered saline, the slides were incubated with anti-mouse $CD4^+/CD8^+$ biotinylated secondary antibodies (Cell & Tissue Staining Kit, R&D Systems, Minneapolis, MN, USA) for 45 min at room temperature. The slides were then washed and immersed in diaminobenzidine chromogen for 10 min. The slides were washed and counterstained with Mayer's hematoxylin. $CD4^+/CD8^+$-stained sections in eight random fields with at least 100 cells/each were counted at 40 × magnifications using a computer screen connected to a microscope (Nikon Eclipse E400, Nikon Corporation, Tokyo, Japan). The cell count was expressed as a percentage of total lymphocytes.

Immunoreactivity of elicited antibodies against viral antigens in sera of viremic HCV patients

Preparation of the immunocomplex

Immune complexes (ICs) were precipitated according to the methods of Lock and Unsworth.[42] Briefly, equal volumes of infection or control sera were mixed with freshly prepared borate buffered saline (25 mM sodium borate, 100 mM boric acid, 75 mM NaCl, 5mM EDTA disodium salt, pH 8.4) containing 7 % polyethylene glycol (PEG-6000), followed by overnight incubation at 4°C and centrifugation at 10,000 *×g* for 20 min. The precipitate was resuspended in 100 µl of 0.1M PBS and stored at -20°C until used.

Immune Assays

The immunoreactivity of mice antisera to ICs was quantitatively assessed using a standard ELISA platform with 0 individual ICs/well and 1:100 diluted mice antisera. The cut-off value for mice antisera immunoreactivity was calculated as the mean absorbance at a wavelength of 450 nm obtained from control mice sera against the precipitated ICs. In addition, western blotting was performed to investigate the pattern of antigenic peptides recognized by the mice antibodies in the precipitated ICs.[37]

Statistical Analysis

The sample size was calculated using G-Power software version 3.1.9.7. The study has four independent groups. The Priori data indicated an approximately 3.037-fold difference in the immunized groups relative to the control groups. Ten mice were allocated to each group to achieve an effect size (f) of 3.037 and a study power of 95% (1-β error probe). A continuity-corrected squared Fisher's exact test was used to evaluate the null hypothesis with a probability of type I error (α- error= 0.05), power = 95%. All the numerical results were analyzed for statistical significance via one-way ANOVA using GraphPad Prism version 9.5.1.

Results

Construction of the HCV-CE vaccine candidate

The synthetic HCV-CE construct was first propagated, purified, and then subjected to two-step verification. First, PCRs were carried out, and the viral core, E1, and E2 fragments were confirmed by visualization on a 1% agarose gel at the expected molecular weights: core ~ 573 bp; E1~576 bp; and E2 ~ 1100 bp (Figure 1A). Subsequently, the full-length HCV-CE fragment was released from the synthetic

clone by double restriction digestion (Figure 1B) and then cloned into both pEGFP-N1 and pET29a expression vectors. The efficiency of cloning was assessed by PCR using purified plasmids prepared from positive transformants grown on 2XYT-ampicillin/kanamycin agar plates using specific core (F) and E2 (R) primers. A homogenous band corresponding to the full-length HCV-CE fragment was visualized at a molecular weight of ~2250 bp, confirming successful cloning of both expression vectors (Figure 1C). The open reading frame of the obtained construct was then confirmed by nucleotide sequence analysis. BLAST results for both nucleotide and translated amino acids revealed partial homology with different sequences published in the National Center for Biotechnology Information (NCBI) database, including those belonging to HCV serotypes 4a, 4m, 4n, 4o, and 4l in addition to genotype 1a, with identity scores ranging between 79.79% and 99.37%. The BLAST results of the translated amino acid sequences against the highest matches of previously published sequences are shown in Figure 1D.

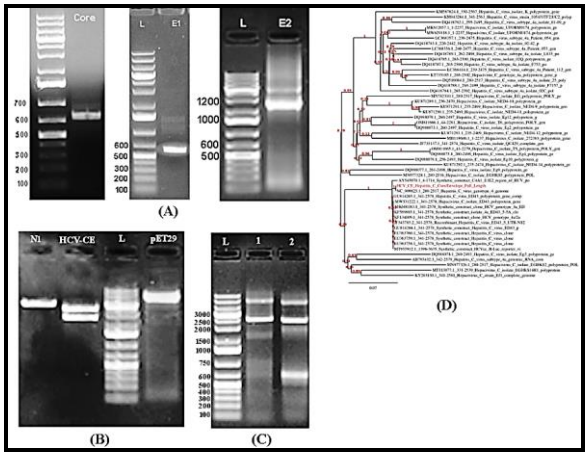

Figure 1. Construction of HCV-CE expression vectors. (A): HCV core, E1, and E2 gene fragments were successfully verified in the synthetic pDrive construct by PCR, as visualized on a 1% agarose gel at the expected molecular weights of 573, 576, and 1100 bp, respectively. The full-length HCV-CE fragment was double digested (B) and then cloned with both pEGFP-N1 and pET29a. Successful cloning was confirmed by PCR using specific core-E2 primers, where the HCV-CE fragment was visualized at the expected Molecular weight (~2250 bp) (C). (D): BLAST results of the HCV-CE translated amino acid sequence against previously published HCV sequences in the NCBI database, with conserved regions shaded in red.

Sequence-based structural analysis of the HCV-CE candidate.

The analysis of the physiochemical parameters of the HCV-CE protein performed by the ProtParam server revealed that it is composed of 746 amino acids with an expected molecular weight of ~ 81.7 kDa. The predicted isoelectric point (PI) was 8.95, and the expected half-life time in mammalian reticulocytes was 30 h (*in vitro*), while it was estimated to be >20 and >10 h in yeast and *E. coli*; respectively (*in vivo*). The instability index score was 36.64, which classifies the vaccine candidate as stable. The high aliphatic index (79.18) in addition to the negative value (-0.041) of the grand average hydrophobicity index further indicated the thermostable nature of the vaccine candidate. The predicted antigenic score of the HCV-CE peptide was 0.4443, which classifies the vaccine candidate as an "antigen", considering that peptides with an antigenic score > 0.4 (cut-off) are generally considered antigenic. In addition, the results of the allergenicity assessment indicated that the vaccine candidate was non-allergen.

Homology modeling and validation of the tertiary structure

The secondary structure analysis of the HCV-CE vaccine construct revealed that it included 25.87% α-helices, 13.4% strands, and 60.73% coils (Figure 2A). Among the top five 3D models predicted by the iterative threading assembly refinement (I-TASSER) server, the model with the highest C score (-2.95) was selected for energy minimization, *i.e.*, refinement. The refined structure (Figure 2B) was first validated through the Protein Structure (ProS)-A web server analysis program, which revealed an overall quality score (Z score) of -7.71 (Figure 2C). Also, the refined modeled structure passed the VERIFY3D evaluation, with 97.72% of the residues having an average 3D-1D score of ≥0.1 and showing high quality (81.1897%) in the ERRAT quality assessing factor. The Ramachandran plot analysis further showed that 99.4% of the model residues fell within the most favored and allowed regions (93.2% in most favored regions, 5.7% in allowed regions, and 0.5% in generously allowed regions) (Figure

2D). Two bad contacts were detected in the predicted model, however, 100% of the planar groups were within the limits.

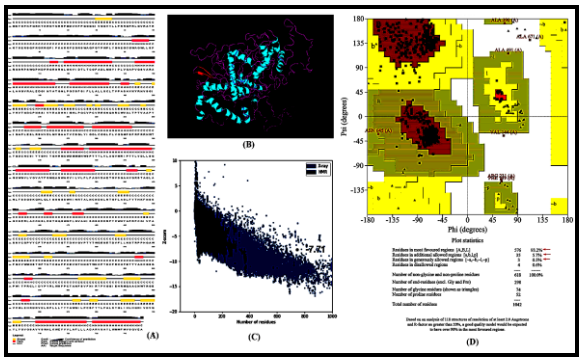

Figure 2. Structure analysis and homology modeling of the HCV-CE vaccine construct. (A): Secondary structure of the HCV-CE peptide. The analysis revealed the presence of 25.87% α-helices, 13.4% strands, and 60.73% coils. (B): Modeled 3Dstructure of the HCV-CE vaccine candidate showing α-helices (cyan), β-sheets (red), and random coils (purple). (C): Validation of the modeled structure using ProsA showing a Z score of -4.28. (D): Ramachandran plot of the 3D model showing 93.2%, 5.7%, and 0.5% of the most favored, allowed, and generously allowed regions; respectively.

Linear and discontinuous B-cell epitope predictions

A total of 25 linear B-cell epitopes were predicted, of which nine were antigenic, four were detected in the primary peptide sequence, and five were detected in the tertiary structure model. Notably, the antigenic epitopes were most common in the core region (4 epitopes), followed by E2 (3 epitopes) and E1 (2 epitopes). The analysis of antigenicity showed that the epitope RTALNCND at position 424-431 (E2) predicted in the primary HCV-CE peptide sequence has the maximum antigenic score (1.5102), followed by the epitope DMMMNWSPTTTLVLA at position 321-335 (E1) predicted in the modeled HCV-CE tertiary structure with an antigenic score of 0.9456 (Supplementary Table 1). In addition, six out of the nine linear epitopes predicted showed IFN-γ induction potential. On the other hand, four discontinuous B-cell epitopes with different sizes ranging from 11-272 residues and a score range of 0.634-0.888 were predicted from the modeled 3D structure (Supplementary Table 2). The predicted epitope located at position 665-746 (E2) had the maximum score (0.888) and highest antigenic score (0.605).

T-cell epitope predictions and population coverage

A total of 93 (9-mer) antigenic cytotoxic T-lymphocyte (CTL) binding epitopes were predicted from the primary HCV-CE peptide sequence, 81 of which were potential binders with different MCH-I alleles. Of these, 42 epitopes showed IFN-γ induction potential (Supplementary Table 4). The epitope RLGVRATRK at position 43-51 (core region) showed a maximum antigenic score of 2.3975, with binding potential to the MCH-I alleles A*03:01, A*30:01, and A*11:01. On the other hand, 28 helper T-lymphocyte (HTL) binding epitopes (15-mer) were predicted, with the lowest IC50 values (higher binding) for the MCH-II alleles HLA-DR, HLA-DQ, and HLA-DP. Of the 28 predicted HTL epitopes, 10 HTL epitopes showed differential antigenic scores and IFN-γ induction potential (Table 5), with the epitope ALKWEYVVLAFLLLA at position 713-727 (E2 region) having the highest antigenic score (1.2602) with binding potential to the MCH-II allele DPA1*02:01/DPB1*01:01. To evaluate the potential cross-reactivity or autoimmunity, all of the predicted T-cell epitopes (10 HTL, 42 CTL) were subsequently used in combination to assess vaccine population coverage. The HCV-CE vaccine candidate was found to cover 96.17% ± 5.21% of the global population, with an average number of epitope hits/HLA combinations recognized by the population estimated at 4.63 ± 1.68 and 2.32 ± 1.17 epitopes recognized by 90% of the global population. The highest and lowest coverage were annotated to North America (100%) and Central America (83.64%), respectively (Figure 3), suggesting the usefulness of this vaccine construct in different regions worldwide. In addition, the results revealed that the CTL epitope/HLA combination FLLLADARV/HLA-A*02:01 and the HTL epitope/HLA combinations LKWEYVVLAFLLLAD, WEYVVLAFLLLADAR/HLA-DP A1*01:03, and HLA-DPB1*02:01 were the most commonly recognized among different regions worldwide.

Epitope conservation

Upon comparing all the B- and T-cell epitopes predicted from the HCV-CE sequence/modeled structure with the corresponding sequences published in the NCBI database, all of the predicted epitopes showed differential degrees of conservation across the reference sequences belonging to different HCV genotypes (Supplementary Tables 1- 4). Notably, most of the linear and all of the discontinuous B cells, as well as the HTL epitopes, showed restricted conservation to the parent genotype (gp4). However, the CTL epitopes FSFRPRRHW, RRGPRLGVR, and LPRRGPRLG at positions 291-299, 39-47, and 37-45, respectively, were highly conserved across almost all HCV genotypes.

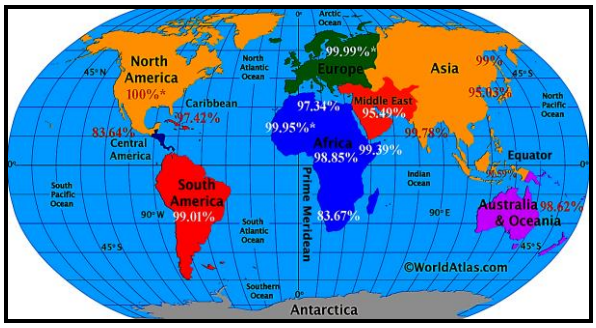

Figure 3. Population coverage of the combined T-cell epitopes predicted from the HCV-CE peptide sequence. The vaccine candidate was found to cover 96.17% ± 5.21% of the global population, with the highest and lowest coverage annotated to North (100%) and Central America (83.64%); respectively.

Molecular docking

The immunoreactivity of the HCV-CE vaccine candidates to the broadly neutralizing antibodies (nAbs) AR3C and HEPC3 was assessed by flexible molecular docking. Based on the lowest energy scores, the best complexes of vaccine candidate-nAbs were selected from the top ten docked complexes. The best HCV-CE–AR3C complex (Model 4) had an energy score of -433.8 kJ/mol, with a center energy (the energy between receptor/nAb and ligand/vaccine) of -446.2 kJ/mol, while the best HCV-CE/HEPC3 complex (Model 1) had an energy score of -412.5 kJ/mol, with a center energy of -460.3 kJ/mol. The interactions between the vaccine candidate and nAbs were visualized using the PyMOL, molecular visualization system, which revealed two hydrogen bonds between the HCV-CE residues ARG606 and ARG639 (donor) and between the AR3C residues HID179 and GLN120 (acceptor), respectively (Figure 4A). Meanwhile, three hydrogen bonds were found in the HCV-CE/HEPC3 complex, two between the HCV-CE residues GLY451 and ARG587 (donor), and the HEPC3 residues THR172 and GLY169 (acceptor), respectively. In addition, another hydrogen bond was detected between the HEPC3 residue SER199 (donor) and the HCV-CE residue GLU591 (acceptor) (Figure 4B). Residues of HCV-CE with polar contacts with the nAb residues are listed in Supplementary Table 5.

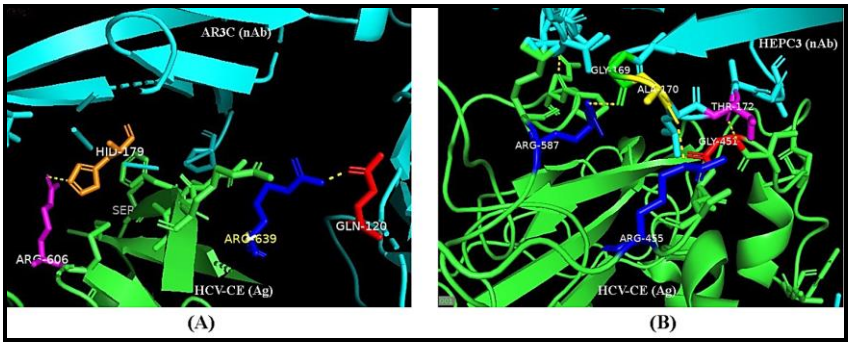

Figure 4. The interactions between residues in polar contact in the docked complexes of the HCV-CE vaccine candidate (green) and AR3C/HEPC3 neutralizing antibodies (blue) are represented in cartoon mode. Two hydrogen bonds (yellow dashes) were detected in the HCV-CE/AR3C complex (A) between the vaccine residues ARG606 and ARG639 (donor) and the AR3C residues HID179 and GLN120 (acceptor); respectively, while three hydrogen bonds were detected in the HCV-CE/HEPC3 complex (B): two bonds between the vaccine residues GLY451 and ARG587 (donor) and the AR3C residues THR172 and GLY169 (acceptor); respectively, in addition to a hydrogen bond was detected between the HEPC3 residue SER199 (donor) and the HCV-CE residue GLU591 (acceptor).

In silico profiling of HCV-CE vaccine immunogenicity

The immunogenicity of the HCV-CE vaccine candidate was evaluated *in-silico* after two injections at 2-week intervals. The run was set for 100 and 400 steps (~34 and 140 days, respectively) to assess the longevity and stability of the elicited immune responses (Figure 5). The introduction of HCV-CE activated different populations of immune cells, where the levels of active B-lymphocytes (Figure 5A) and cytotoxic T-lymphocytes (CTLs) (Figure 5C) dramatically increased after booster immunization. The number of active B lymphocytes reached their magnitude and remained stable for up to 134 days (Figure 5B), suggesting the generation of memory B cells, while the number of CTLs reached its maximum after 60 days before decreasing to its minimum after 120 days (Figure 5D). Two peaks of antigen-presenting B-cell populations were observed during the first week after the primary dose, reflecting early seroconversion, and following the second dose on the 15th day (black line, Figure 5A). Similarly, the levels of active and duplicating helper T-lymphocytes (HTL) were dramatically upregulated after the second dose (Figure 5E), reaching their magnitude after 22 days before declining to the lowest level after 80 days (Figure 5G). Notably, the main population affected by active HTL was Th1 (>90% of the total population), while the levels of immunosuppressive and regulatory Th2 and Th17, respectively, approached zero % (Figures 5F, 5H). The simulation results also revealed that the HCV-CE immunogen elicited robust humoral and cellular responses, where the levels of immunoglobulins reached the maximum level after the second dose and remained detectable for up to 120 days (Figures 5I, 5J), concomitant with a remarkable level of IFN-γ that persisted for up to 50 days (Figures 5K, 5L). As indicated in the inset plots of the same figures, the upregulation of IL-2 (orange line) after the second dose reflects the ability of the HCV-CE vaccine candidate to induce T-cell proliferation, whereas the low Simpson diversity index of clonal specificity (D-index, blue line) suggests the diversity of elicited immune responses.

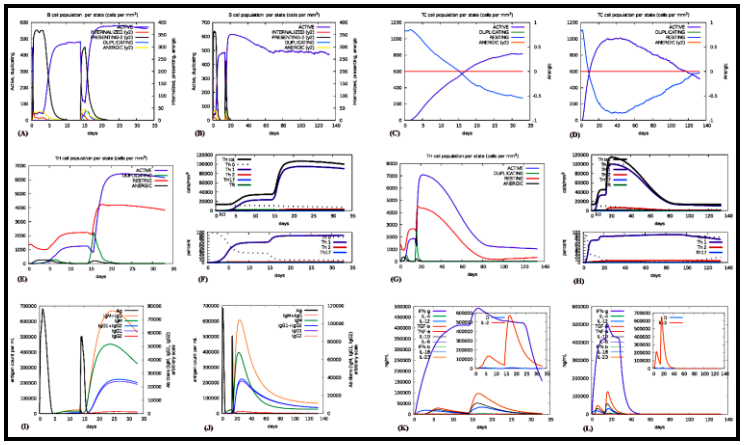

Figure 5. *In-silico* profiling of HCV-CE vaccine immunogenicity after two immunizations at 2-week intervals. The introduction of the HCV-CE vaccine elicited the activation and proliferation of different immune cells. The numbers of active B- (A) and cytotoxic T cells (C) increased after the second dose; in particular, the numbers of both antigen-presenting B cells and memory cells remained detectable for 134 and 120 days, respectively (B, D). The active and duplicated HTLs (mainly Th1) reached their maximum level after 22 days and remained detectable for up to 80 days (E-H). The vaccine candidate also induced robust humoral and cellular responses, as demonstrated by high levels of immunoglobulins that persisted for ~ 120 days (I, J) and remarkable levels of IFN-γ that remained detectable for ~ 50 days (K, L). The high levels of IL-2 (orange line) shown in the inset plot in Figures K and L indicate the potential of the HCV-CE vaccine candidate to induce the proliferation of T cells, while the minimal D-index (blue line) suggests its potential to induce diverse immune responses.

Expression of HCV-CE recombinant protein

The protein expression level was assessed in terms of total protein content (mg/ml). The total amount of total crude recombinant HCV-CE protein obtained was estimated to be 1.204 mg/mL, while the amount of total purified protein obtained was estimated to be 0.951 mg/100 mL culture, *i.e.*, 9.51 mg/L. After the crude and purified protein preparations were profiled via SDS–PAGE (Figure 6A), several recombinant proteins with different molecular weights were observed in the crude protein preparation, with a prominent band at a molecular weight of ~ 80 kDa corresponding to the expected molecular weight of the full-length HCV-CE protein detected in both the crude and purified preparations. Successful protein expression was further confirmed by western blotting (Figure 6B) using sera from viremic HCV patients as a source of detector antibodies, where an immunogenic band corresponding to the full-length HCV-CE protein was visualized at molecular weight of 80 kDa.

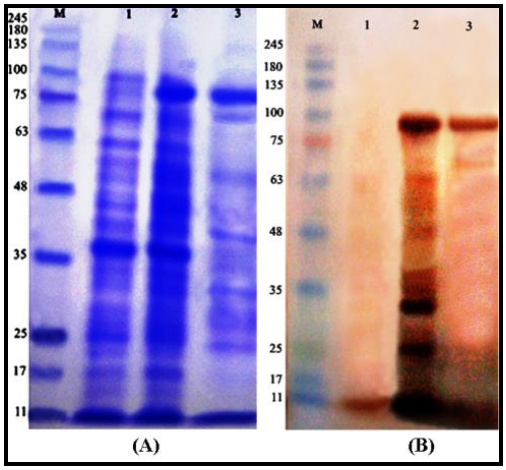

Figure 6. Characterization of recombinant HCV-CE protein expression in *E. coli* BL21 (DE3). (A): 14% SDS–PAGE showing the profile of HCV-CE recombinant *E. coli* BL21 (DE3) cell lysates, where a prominent band was visualized at Molecular weight of ~80 kDa in recombinant protein preparations corresponding to the expected Molecular weight of full-length HCV-CE peptide. Lane (M) refers to the pre-stained protein marker (11-245 kDa); lane (1) refers to the uninduced culture; and lanes (2) and (3) refer to crude and purified HCV-CE protein preparations; respectively. (B): Western blot showing the reactivity of crude (lane C) and purified (lane P) HCV-CE proteins against the pooled sera of viremic HCV patients, where the immunogenic band of the HCV-CE peptide was visualized at a Molecular weight of ~80 kDa.

Immune responses elicited in animals immunized with different vaccine combinations

All immunized animals showed an IgM response as early as 7 days after the primary dose, and seroconversion was maximized by the 14th day with a progressive decrease in IgM levels. After the booster dose, the IgG levels in the vaccinated animals continued to increase, reaching their magnitude by the 28th day, where the DNA/DNA- and DNA/protein-immunized animal groups showed 88.09 and 78.96% higher IgG levels than the first and third weeks, respectively (p<0.0001), while the DNA/protein-immunized animals (Figure 7B) showed 84.85 and 54.91% higher IgG levels at the same time points, respectively (p<0.0001). Notably, compared with those in DNA/DNA-vaccinated animals, the IgG levels in DNA/protein-immunized animals were 1.68-fold greater in the third week, however, the IgG levels in DNA/DNA-immunized animals were 17.4% higher than those in DNA/protein-immunized animals in the fourth week (p= 0.0201) (Figures 7A, 7B). At the cellular level, HCV-CE immunization also had a positive effect on the spleen indices of immunized animals. Both the DNA/DNA-immunized group and the DNA/protein-immunized group had significantly higher spleen indices than did the control groups (PBS, vacant pEGFP-N1-immunized animals) (p<0.0001 and p=0.0003, respectively). However, no significant difference was observed between the control groups (Figure 7C). Similarly, all of the immunized animals elicited robust cellular responses, as indicated by significantly higher counts of peripheral and splenic $CD4^+$ and $CD8^+$ lymphocytes in the immunized animals than in the control animals. DNA/DNA and DNA/protein-immunized animals had 1.54- and 1.75-fold (p= 0.0164 and p=0.0065) and 2.52-and 2.14-fold (p<0.0001 for both) higher peripheral $CD4^+$ and $CD8^+$ counts, respectively (Figures 7D, 7E). While they had 2.15-, 1.77- and 1.91-and 2.26-fold higher splenic $CD4^+$ and $CD8^+$ counts, respectively (p<0.0001 for both) (Figures 7F, 7G). Despite the absence of a significant difference, the peripheral $CD4^+$ cell count was slightly higher in DNA/protein-immunized animals than in those

immunized with the DNA/DNA combination, while the opposite trend was observed for the splenic population (p= 0.0066) (Figures 7D, 7F). Meanwhile, the DNA/DNA immunization elicited greater numbers of peripheral and splenic $CD8^+$ cells (p= 0.0005 and p=0.0238, respectively) than did DNA/protein immunization (Figures 7E, 7G). These results were further confirmed by immunostaining of spleen sections (Figure 7H) that revealed significantly higher percentages of both splenic $CD4^+$ and $CD8^+$ cells in the spleens of DNA/DNA-immunized animals (60 and 90%, p=0.0009 and p=0.0185, respectively) (Figure 7, H3 and H7) than in those of DNA/protein-immunized animals (45 and 80%; respectively) (Figure 7, H4 and H8). Notably, the percentages of splenic $CD4^+$ and $CD8^+$ cells in both immunized groups were significantly higher than those in the PBS (30 and 50%, respectively) (Figure 7, H.1 and H.5) and pEGFP-N1 (32 and 51%, respectively) (Figure 7, H2 and H6) control groups (p<0.001). Additionally, IFN-γ, IL-10 and TNF-α levels were greater in all immunized animals than in the control animals (p<0.0001, for all). Compared with DNA/protein-immunized animals, DNA/DNA-immunized animals were found to have significantly higher levels of IFN-γ and TNF-α (p<0.0001, for each) and lower levels of IL-10 (p=0.0331) (Figure 7I), while no significant difference was detected between the control groups.

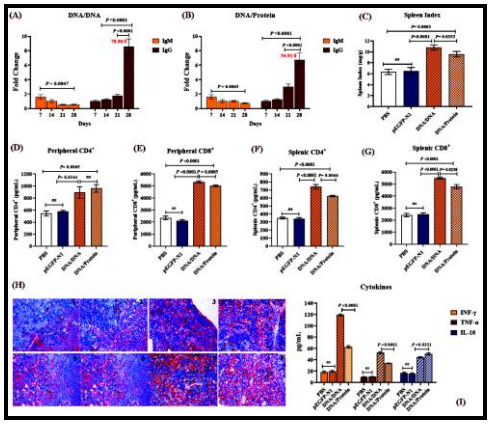

Figure 7. Profiling the immune responses elicited in animals immunized with different HCV-CE vaccine combinations. At the end of the experimental period, DNA/DNA-immunized animals (A) had IgG levels that were 88.09% and 78.96% higher than those at the 1st and 3rd weeks, respectively (p<0.0001), while DNA/protein-immunized animals (B) had IgG levels that were 84.85 and 54.91% higher at the same time points; respectively (p<0.0001). DNA/DNA immunization produced a significantly higher spleen index relative to both the control and DNA/protein combination (p<0.0001 and p=0.0353, respectively) (C). Compared to DNA/DNA-immunized animals, those immunized with the DNA/protein combination showed a slightly higher level of peripheral $CD4^+$cells despite the absence of a significant difference (D); however, they showed significantly higher peripheral $CD8^+$ (p=0.0005) (E) and splenic $CD4^+$ and $CD8^+$ counts (p= 0.0066, and p=0.0238, respectively) (F, G). The results of immunostaining (H) confirmed these results, as both immunized groups showed higher counts of splenic $CD4^+$ and $CD8^+$ cells than did the PBS (30% and 50%; respectively) (H.1 and H5) and pEGFP-N1 (32 and 51%, respectively) (H.2 and H6) control groups (p<0.001). Spleen sections from DNA/DNA-immunized animals showed significantly higher counts of splenic $CD4^+$ and $CD8^+$cells (60 and 90%, p= 0.0009 and p=0.0185, respectively) (H.3, and H7) than did those from DNA/protein-immunized animals (45, 80%; respectively) (H.4 and H8). Both vaccinated groups showed significantly higher levels of circulating cytokines than did the control groups (p<0.0001), with DNA/DNA-immunized animals having significantly higher levels of IFN-γ (p<0.0001) and TNF-α (p<0.0001) and lower levels of IL-10 (p=0.0331) than DNA/protein-immunized animals (I).

Elicited antibodies capture native viral antigens in sera of viremic HCV patients

The ability of anti-HCV-CE antibodies elicited in immunized animals to capture native viral antigens in immunocomplex prepared from sera of HCV patients was tested by a standard ELISA platform. The anti-HCV-CE antibodies of all immunized animal groups were able to recognize the circulating viral antigens in 100% of the tested ICs (Figure 8A), despite the higher levels in samples screened with sera from DNA/DNA-vaccinated animals than in those from DNA/protein-vaccinated animals (p<0.0001). The immunoreactivity of the mice antibodies was further confirmed by western blotting, which revealed different patterns of immunogenic bands, with molecular weights

ranging between 25-245 and 21-245 kDa as detected by anti-HCV-CE obtained from the DNA/DNA- and DNA/protein-immunized mice, respectively (Figure 8B). Notably, prominent immunogenic bands recognized by the anti-HCV-CE obtained from the DNA/DNA-vaccinated group were visualized at molecular weights of ~25, 40, 62, and 90 kDa, whereas the antibodies obtained from DNA/protein-immunized mice showed prominent bands at molecular weights of ~21, 22, 33, and 83 kDa that might correspond to the predicted molecular weights of the same antigens, respectively. These bands might correspond to the core, E1, E2, and full-length E1-E2, respectively, while the high molecular weight. band visualized at ~250 kDa might account for the recognition of the E1-E2 epitopes expressed on the whole viral particles.

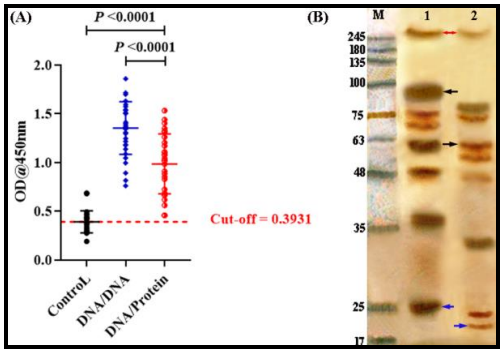

Figure 8. Mice anti-HCV-CE capture circulating viral antigens in immunocomplex prepared from the sera of viremic HCV patients. (A): Scatter plot of the optical density values at 450 nm (OD450) of circulating viral antigens (immunocomplex, IC) prepared from the sera of viremic HCV patients treated with anti-HCV-CE obtained from immunized mice. The mean OD_{450} of the anti-HCV-CE antibody obtained from DNA/DNA-immunized animals was significantly higher than that of the anti-HCV-CE antibody obtained from DNA/DNA-immunized animals ($p<0.0001$), and both groups exhibited significantly higher values than did the control group (unimmunized) ($p<0.0001$). (B) Western blot of ICs prepared from pooled HCV-patients' sera recognized by anti-HCV-CE antibodies obtained from DNA/DNA-immunized animals (lane 1) and DNA/protein-immunized animals (lane 2). Prominent immunogenic bands were visualized at molecular weights of ~25, 40, 62, and 90 kDa and ~21, 22, 33, and 83 kDa recognized by anti-HCV-CE obtained from both groups; respectively, which might correspond to the core (blue arrow), E1, E2, and full-length E1-E2 (black arrows); respectively. The high Molecular weight. The bands at ~250 kDa might correspond to E1-E2 epitopes expressed on whole viral particles.

Discussion

Despite the previous findings of suboptimal immune responses induced by full-length envelope protein-based HCV vaccines, whether as DNA or VLP immunogens, the incorporation of unfavorable regions such as HVR1 reportedly occludes the conserved epitopes of broadly neutralizing antibodies and impairs viral neutralization.[14,43] However, other reports showed that multiple epitope-based vaccines can induce complementary neutralizing breadth and probably antiviral neutralizing synergism.[44] Therefore, in this study a chimeric DNA construct encoding full-length HCV structural gene fragments was designed, aiming to utilize the various conformational B-cell epitopes expressed on viral antigens, considering that most broadly neutralizing anti-HCV antibodies recognize overlapping clusters of conformational epitopes expressed on different structural and non-structural viral proteins.[45-47] The construction of our vaccine candidate was confirmed by specific amplification of the inserted genes and by BLAST analysis of nucleotide and translated amino acid sequences that revealed a high degree of similarity with several viral serotypes of genotype 4 as well as different genotypes (1a, 1b), suggesting potential cross-genotype reactivity of the vaccine candidate.

In the context of vaccine design, protein stability, hydrophobicity, and folding are crucial determinants of the biochemical and immunological characteristics of the candidate immunogen.[48] This information could be particularly useful for optimizing the expression of a given immunogen. In this report, the translated amino acid sequence of the HCV-CE fragment was subjected to structural analyses that revealed remarkable stability/thermo-stability after expression, with half-life time >10 and 30 h in bacterial and mammalian cells, respectively. Moreover, the antigenicity and allergenicity assessments indicated that the vaccine candidate is antigenic and non-

allergenic, which primarily confirmed its safety as an immunogen. Accordingly, the platform for bacterial expression was optimized to maximize the yield of recombinant HCV-CE protein and overcome the reported toxicity of the E1/E2 domain.[49] Using a T7 promoter-based expression vector in C41(DE3) cells that enables the overexpression of toxic proteins yielded a total of 9.51 mg/L,[50] which surpassed that previously reported by Shawky et al., 2015.[37] The recombinant protein expression was further confirmed by SDS–PAGE, which revealed good expression of the full-length HCV-CE protein as a homogenous band visualized at the expected molecular weight, and western blot using sera from viremic HCV-patients as a source of detector antibodies. This indicated that the specific antigenicity of the expressed protein was demonstrated as a prominent immunogenic band corresponding to the expected size.

The modeled tertiary structure showed high scores in validation assessments, with an excellent quality score (Z score) of -7.71. This suggests that the predicted model falls within the score range of native proteins of the same structure experimentally determined by X-ray and nuclear magnetic resonance crystallography and has 99.4% of residues within the most favored/allowed regions and 100% of the planar groups within the limits in the Ramachandran plot.

Several epitopes with differential antigenic scores and the potential to induce IFN-γ were predicted. Of the 25 linear B-cell epitopes, 9 epitopes predicted to be effective antigenicity were distributed as four predicted from the primary peptide sequence and five predicted from the modeled 3D structure. Additionally, four conformational B-cell epitopes of different sizes were predicted from the modeled 3D structure, three of which were located in the E2 region, with the epitope at position 423-571 including the conserved CD81-binding loop reportedly targeted by the majority of broadly neutralizing antibodies against HCV.[51-53] Interestingly, 52.54% of the peptide residues fell within the conformational epitopes, suggesting the high potential of this vaccine candidate for producing a proficient antibody-mediated antiviral response. On the other hand, 42 out of 93 CTL (9-mer) and 10 out of 28 HTL (15-mer) epitopes were predicted, all were potential antigens and IFN-γ inducers. Notably, all of the predicted epitopes were highly conserved across HCV genotypes. While all of the predicted B- and HTL epitopes were exclusively conserved in the parent genotype 4. Of the 42 predicted CTL epitopes, 16 epitopes showed high conservation in other genotypes, with two epitopes in the core region with high antigenic scores conserved in almost all HCV genotypes.

Typically, T-lymphocytes recognize a specific major histocompatibility complex (MHC) molecule complexed with a particular epitope. In other words, a given epitope would induce a response only in individuals who express the MHC molecule compatible with this particular epitope. Since MHC molecules are highly polymorphic,[54] with more than a thousand different human MHC (human leukocyte antigen, HLA) alleles identified thus far, selecting multiple antigen-based vaccines with different HLA-binding specificities would enable wider coverage of the targeted populations. However, this assumption is complicated by the reportedly high MHC polymorphism, where the expression of HLA serotypes occurs at dramatically variable frequencies among different ethnicities, which eventually leads to diverted immune responses or generates autoimmune-triggered cross-reactivity.[55,56] To evaluate the likelihood of HCV-CE generating unfavorable immune responses, the predicted HTL and CTL epitopes were used in combination with HLA serotypes to assess their population coverage. The vaccine candidate was found to cover 96.17% of the global population without any homologs of the selected epitopes found in humans, which nullifies the propensity to produce cross-reactivity. These findings suggest the use of these epitopes as good targets of antiviral agents and prophylactic vaccine approaches against multiple HCV genotypes in different regions worldwide and further support the aforementioned hypothesis about the potential cross-genotype reactivity of the proposed vaccine candidate.

Molecular docking revealed good interactions between the vaccine candidate and

the broadly neutralizing antibodies AR3C and HEPC3. As, several polar interactions in addition to multiple hydrogen bonds were detected between the residues of HCV-CE and both nAbs (AR3C and HEPC3), which significantly contributed to the anticipated antiviral response. The immunoreactivity of the vaccine candidate was further profiled *in-silico* through immune simulation. This revealed the potential of HCV-CE to induce long-lasting humoral and cellular responses that were maximized after booster immunization, as demonstrated by the presence of active and/or replicating B-cells and CTL/HTL cells, high levels of immunoglobulins that might remain detectable for up to 4 months, and robust production of IL-2 and IFN-γ with undetectable levels of the anti-inflammatory cytokines IL-10 and TGF-β. Significantly, more than 90% of active HTLs were Th1, while the levels of immunosuppressive and regulatory Th2/Th17 cells approached zero%.

The pattern of immune responses elicited in animals immunized with different vaccine combinations approached that was *in-silico* profiled, where both immunized groups showed detectable levels of immunoglobulins during the first week and seroconversion was maximized after the second dose. Despite the slower progression of IgG levels observed in DNA/DNA-immunized animals relative to those immunized with DNA/protein combination. This is largely attributed to the initially limited availability of antigens expressed in DNA vaccines.[57] However, the IgG levels were upregulated with progressive antigen expression concomitant with the generation of memory cells, showing ultimate IgG levels that exceeded those in protein-boosted animals. These results are not surprising though, given that the DNA construct expresses the E1/E2 antigens in their native form, *i.e.*, a glycosylated tertiary structure, which might have induced a humoral response against both conformational and linear epitopes, unlike the recombinant protein that includes only linear epitopes. Similarly, compared with DNA/protein combination immunization, DNA/DNA immunization had a significantly stronger effect on the splenic index, as demonstrated by higher levels of peripheral and splenic $CD4^+$ and $CD8^+$ T lymphocytes, which was further confirmed by immunostaining of splenic sections. The protein-boosted animals, however, showed slightly higher levels of peripheral $CD4^+$ cells despite the absence of a significant difference, which is largely attributable to the inherently antigenic nature of recombinant proteins such as immunogens that typically induce higher levels of memory $CD4^+$.[58] Nonetheless, the superior effect of DNA/DNA immunogens on cellular immunity was further confirmed in terms of the remarkable production of IFN-γ, which accounts for the differentiation and recruitment of effector $CD4^+$ T lymphocytes,[59] significantly higher levels of TNF-α, and lower levels of IL-10 relative to DNA/protein combinations. Taken together, these findings strongly suggest that the high propensity of HCV-CE to produce a Th1-skewed immune response is critical for controlling HCV infection.[60] Our findings, however, contradict the previously reported stronger immunogenicity of the DNA prime-boost regimen attributable to boosting with recombinant rather than DNA or VLP-expressed E1/E2 peptides.[25] Unlike our study, Masavuli et al., 2019[24] used a secreted oligomerized peptide that lacks the E1-E2 transmembrane domain for boosting, therefore, the immunogenicity of the secreted peptides could be rationally enhanced since the unfavorable immunogenic effect of HVR1 falling within these domains was primarily abrogated.

The main limitation of this study was the unavailability of a proper replication system for assessing the neutralizing activity of elicited anti-HCV-CE antibodies. However, their ability to recognize/capture the native viral antigens in immunocomplex prepared from viremic HCV patient sera was assessed by ELISA, which revealed 100% recognition of all tested samples despite the higher absorbance values observed at OD_{450} in samples screened with DNA/DNA-vaccinated animal sera, largely attributable to their recognition of conformational epitopes on the corresponding antigens. Furthermore, the immunoreactivity of anti-HCV-CE was further assessed by western blotting, which revealed heterogeneous profiles of immunogenic bands

recognized by the antibodies obtained from both vaccinated groups. In detail, prominent immunogenic bands that might account for the expected sizes of the viral core, E1, E2, and the full-length core-E1-E2 peptide recognized by the anti-HCV-CE obtained from DNA/DNA were observed at higher molecular weights relative to those captured by antibodies from DNA/protein-immunized animals. As the antibodies of the former were mainly directed against the conformational structure of the vaccine candidate, in which both E1/E2 fragments were typically subjected to post-translational glycosylation, the higher apparent molecular weight of the immunogenic bands can be expected as the antibodies recognized the native antigens in patients' immunocomplex, while those of the protein-boosted animals recognized only the linear epitopes expressed on the individual antigens and the whole viral particles, which indicates that the high molecular weight band was recognized by both antibody preparations. In addition, these findings reflect the ability of anti-HCV-CE elicited in mince immunized with the DNA construct based on the original ED43 strain to cross-neutralize bacterially expressed antigens originating from a different (recent) isolate, which confirms the high epitope conservation across the two isolates used.

In conclusion, despite the lack of consensus on the inability of HCV vaccine candidates available to provide sterilizing immunity, the reduction in primary viremia might allow timely induction of cellular immunity, which is crucial for viral clearance. Despite the limited evaluation of the neutralizing capacity of the proposed vaccine, its promising potential regarding safety, immunogenicity, and population coverage represents a new perspective of full-length protein-based DNA vaccines against HCV that is worthy of further assessment.

Acknowledgements

The authors acknowledge the National Research Centre (NRC) of Egypt for providing all needed facilities and logistics for the work. The authors also acknowledge the GI/Hepatology Specialist Dr. Yasser K. Elesnawy at the Viral Hepatitis Clinic, El-Gomhouria Teaching Hospital-Cairo, Egypt, for his kind assistance in collecting the viremic HCV patient samples. Special thanks to Dina Mofed (University of Science and Technology, Zewail City of Science and Technology) for her help and support in this work.

Author Contributions

EAS, contributed to the data collection, methodology, and preparation of the manuscript. AT contributed to conception, revision for important intellectual content, supervision, and preparation of the manuscript. TZS, YSE, RE, SS, contributed to the study conception, revision of important intellectual content, and supervision. HS, contributed to conception, revision for important intellectual content, supervision, and preparation of the manuscript. All authors equally contributed to editing/reviewing the final manuscript.

Declaration of Conflicting Interests

The author(s) declared no potential conflicts of interest with respect to the research, authorship, and/or publication of this article.

Funding

This work was primarily supported by the NRC in the context of the Ph.D. funding provided to Eman A. Salem under the supervision of Prof. Ashraf A. Tabll. Additionally, the codon-optimized HCV-CE fragment, pEGFP-N1 vector, and the molecular characterization experiments were supported by Prof. Tamer Z. Salem in the context of his project (Science and Technology Development Fund, Grand/Award Number: 22976), while the immunological assessments were supported by Prof. Yasmine S. El-Abd through her internal project funded by the NRC [Project ID: 12010130].

Ethical Approval

The study protocol including the use of an animal model and the human sera was reviewed and approved by the Medical Research Ethics Committee of the National Research Center, Egypt in 2017 (Approval NO: 17121). The human sera were collected from the Viral Hepatitis Unit in El-Gomhouria Teaching Hospital. Sera were coded and anonymously preserved at -20 °C until used.

Electronic Supplementary Material

The electronic supplementary material is available in Supplementary Data File.

References

1. World Health Organization. WHO fact sheet: Hepatitis C, 9 April (2024). Available from: https://www.who.int/news-room/fact-sheets/detail/hepatitis-c [Accessed 13 May 2024].
2. Sarrazin C (2021). Treatment failure with DAA therapy: Importance of resistance. *J Hepatol.* 74(6):1472-1482. https://doi.org/10.1016/j.jhep.2021.03.004
3. Di Stefano M, Faleo G, Farhan Mohamed AM, et al. (2020). *New Microbiol*.; 44(1):12-18.
4. Hajarizadeh B, Cunningham EB, Valerio H, Martinello M, et al. (2021). Hepatitis C reinfection after successful antiviral treatment among people who inject drugs: A meta-analysis. *J Hepatol.* 72(4):643-657. https://doi.org/10.1016/j.jhep.2019.11.012
5. Franco S, Tural C, Nevot M, et al. (2014). Detection of a sexually transmitted hepatitis C virus protease inhibitor-resistance variant in a human immunodeficiency virus-infected homosexual man. *Gastroenterology.* 147(3):599-601.e1. https://doi.org/10.1053/j.gastro.2014.05.010
6. Midgard H, Bjøro B, Mæland A, et al. (2016). Hepatitis C reinfection after sustained virological response. *J Hepatol.* 2016; 64(5):1020-1026. https://doi.org/10.1016/j.jhep. 2016.01.001
7. Martell M, Esteban JI, Quer J, et al. (1992). Hepatitis C virus (HCV) circulates as a population of different but closely related genomes: quasispecies nature of HCV genome distribution. *J Virol.* 66(5):3225-9. https://doi.org/10.1128/jvi.66.5.3225-3229.1992
8. Malekshahi A, Alamdary A, Safarzadeh A, et al. (2023). Potential roles of core and core +1 proteins during the chronic phase of hepatitis C virus infection. *Future Virol.* 18(3). https://doi.org/10.2217/fvl-2022-0117
9. Kanda T, Steele R, Ray R, et al. (2008). Hepatitis C virus core protein augments androgen receptor-mediated signaling. *J Virol.* 82(22):11066-72. https://doi.org/10.1128/jvi.01300-08
10. Zhu W, Chang Y, Wu C, et al. (2010). The wild-type hepatitis C virus core inhibits initiation of antigen-specific T- and B-cell immune responses in BALB/c mice. *Clin Vaccine Immunol.* 17(7):1139-47. https://doi.org/10.1128%2FCVI.00490-09
11. Tarr AW, Khera T, Hueging K, et al. (2015). Genetic Diversity Underlying the Envelope Glycoproteins of Hepatitis C Virus: Structural and Functional Consequences and the Implications for Vaccine Design. *Viruses.* 7(7):3995-4046. https://doi.org/10.3390/v7072809
12. Taylor DR, Shi ST, Romano PR, et al. (1999). Inhibition of the interferon-inducible protein kinase PKR by HCV E2 protein. *Science.* 285(5424):107-110. https://doi.org/10.1126/science.285.5424.107
13. Ray SC, Wang YM, Laeyendecker O, et al. (1999). Acute hepatitis C virus structural gene sequences as predictors of persistent viremia: hypervariable region 1 as a decoy. *J Virol.* 73(4):2938-46. https://doi.org/10.1128/jvi.73.4.2938-2946.1999
14. Quarleri JF, OubiñaJR (2016). Hepatitis C virus strategies to evade the specific-T cell response: a possible mission favoring its persistence. *Ann Hepatol.* 15(1):17-26. https://doi.org/10.5604/16652681.1184193
15. Broering TJ, Garrity KA, Boatright NK, et al. (2009). Identification and characterization of broadly neutralizing human monoclonal antibodies directed against the E2 envelope glycoprotein of hepatitis C virus. *J Virol.* 83(23):12473-82. https://doi.org/10.1128/jvi.01138-09
16. Owsianka AM, Tarr AW, Keck ZY, Li TK, Witteveldt J, Adair R, Foung SKH, Ball JK, Patel AH. Broadly neutralizing human monoclonal antibodies to the hepatitis C virus E2 glycoprotein. J Gen Virol. 2008; 89(Pt 3):653-659. https://doi.org/10.1099/vir.0.83386-0
17. Fauvelle C, Colpitts CC, Keck ZY, Pierce BG, Foung SK, Baumert TF. Hepatitis C virus vaccine candidates inducing protective neutralizing antibodies. Expert Rev Vaccines. 2016; 15(12):1535-1544. https://doi.org/10.1080/14760584.2016.1194759
18. Zhu F, Wang Y, Xu Z, et al. (2019). Novel adeno-associated virus-based genetic vaccines encoding hepatitis C virus E2 glycoprotein elicit humoral immune responses in mice. *Mol Med Rep.* 19(2):1016-1023. https://doi.org/10.3892/mmr.2018.9739
19. Johnson J, Freedman H, Logan M, et al. (2019). A Recombinant Hepatitis C Virus Genotype 1a E1/E2 Envelope Glycoprotein Vaccine Elicits Antibodies That Differentially Neutralize Closely Related 2a Strains through Interactions of the N-Terminal Hypervariable Region 1 of E2 with Scavenger Receptor B1. *J Virol.* 29; 93(22):e00810-19. https://doi.org/10.1128/jvi.00810-19
20. Cox AL (2020). Challenges and Promise of a Hepatitis C Virus Vaccine. *Cold Spring Harb*

Perspect Med. 10(2):a036947. https://doi.org/10.1101%2Fcshperspect.a036947

21. Hartlage AS, Murthy S, Kumar A, et al. (2019). Vaccination to prevent T cell subversion can protect against persistent hepacivirus infection. *Nat Commun.* 10(1):1113. https://doi.org/10.1038/s41467-019-09105-0
22. Olivera S, Perez A, Falcon V, et al. (2020). Protective cellular immune response against hepatitis C virus elicited by chimeric protein formulations in BALB/c mice. *Arch Virol.* 165(3):593-607. https://doi.org/10.1007/s00705-019-04464-x
23. Shayeghpour A, Kianfar R, Hosseini P, et al. (2021). Hepatitis C virus DNA vaccines: a systematic review. *Virol J.* 18(1):248. https://doi.org/10.1186/s12985-021-01716-8
24. Masavuli MG, Wijesundara DK, Underwood A, et al. (2019). A Hepatitis C Virus DNA Vaccine Encoding a Secreted, Oligomerized Form of Envelope Proteins Is Highly Immunogenic and Elicits Neutralizing Antibodies in Vaccinated Mice. *Front Immunol.* 10:1145. https://doi.org/10.3389/fimmu.2019.01145
25. Wilkins MR, Gasteiger E, Bairoch A, et al. (1999). Protein identification and analysis tools in the ExPASy server. *Methods Mol Biol.* 112:531-52. https://doi.org/10.1385/1-59259-584-7:531
26. Doytchinova IA, Flower DR (2007. VaxiJen: a server for prediction of protective antigens, tumour antigens and subunit vaccines. *BMC Bioinformatics.* 8:4. https://doi.org/10.1186/1471-2105-8-4
27. Dimitrov I, Bangov I, Flower DR, et al. (2014). AllerTOP v.2--a server for in silico prediction of allergens. *J Mol Model.* 20(6):2278. https://doi.org/10.1007/s00894-014-2278-5
28. El-Manzalawy Y, Dobbs D, Honavar V (2008). Predicting linear B-cell epitopes using string kernels. *J Mol Recognit.* 21(4):243-55. https://doi.org/10.1002/jmr.893
29. Kringelum JV, Lundegaard C, Lund O, et al. (2012). Reliable B cell epitope predictions: impacts of method development and improved benchmarking. *PLoS Comput Biol.* 8(12):e1002829. https://doi.org/10.1371/journal.pcbi.1002829
30. Vita R, Mahajan S, Overton JA, et al. (2019). The Immune Epitope Database (IEDB): 2018 update. *Nucleic Acids Res.* 8; 47(D1):D339-D343. https://doi.org/10.1093/nar/gky1006
31. Larsen MV, Lundegaard C, Lamberth K, et al. (2007). Large-scale validation of methods for cytotoxic T-lymphocyte epitope prediction. *BMC Bioinformatics.* 8:424. https://doi.org/10.1186/1471-2105-8-424
32. Shahid F, Ashfaq UA, Javaid A, et al. (2020). Immunoinformatics guided rational design of a next generation multi epitope based peptide (MEBP) vaccine by exploring Zika virus proteome. *Infect Genet Evol*. 80:104199. https://doi.org/10.1016/j.meegid.2020.104199
33. Vita R, Zarebski L, Greenbaum JA, et al. (2010) The immune epitope database 2.0. *Nucleic Acids Res.* 38(Database issue):D854-62. https://doi.org/10.1093/nar/gkp1004
34. Bui HH, Sidney J, Dinh K, et al. (2006). Predicting population coverage of T-cell epitope-based diagnostics and vaccines. *BMC Bioinformatics.* 7:153. https://doi.org/10.1186/1471-2105-7-153
35. Morris GM, Huey R, Lindstrom W, et al. (2009). AutoDock4 and AutoDockTools4: Automated docking with selective receptor flexibility. *J Comput Chem.* 30(16):2785-91. https://doi.org/10.1002/jcc.21256
36. Rapin N, Lund O, Bernaschi M, et al. (2010). Computational immunology meets bioinformatics: the use of prediction tools for molecular binding in the simulation of the immune system. *PLoS One.* 5(4):e9862. https://doi.org/10.1371/journal.pone.0009862
37. Shawky H, Maghraby AS, Solliman Mel-D, et al. (2015). Expression, immunogenicity and diagnostic value of envelope proteins from an Egyptian hepatitis C virus isolate. *Arch Virol.* 160(4):945-58. https://doi.org/10.1007/s00705-015-2334-1
38. Laemmli UK (1970). Cleavage of structural proteins during the assembly of the head of bacteriophage T4. *Nature.* 227(5259):680-5. https://doi.org/10.1038/227680a0
39. Towbin H, Staehelin T, Gordon J. (1979). Electrophoretic transfer of proteins from polyacrylamide gels to nitrocellulose sheets: procedure and some applications. *Proc Natl Acad Sci U S A.* 76(9):4350-4. https://doi.org/10.1073/pnas.76.9.4350
40. Li X, Wu Z, He B, Zhong W et al. (2018). Tetrandrine alleviates symptoms of rheumatoid arthritis in rats by regulating the expression of cyclooxygenase-2 and inflammatory factors. *Exp Ther Med.*16(3):2670-2676. https://doi.org/10.3892%2Fetm.2018.6498
41. Engvall E, Perlmann P (1971). Enzyme-linked immunosorbent assay (ELISA). Quantitative assay of immunoglobulin G. *Immunochemistry.*

8(9):871-4. https://doi.org/10.1016/0019-2791(71)90454-x

42. Lock RJ, Unsworth DJ (2000) Measurement of immune complexes is not useful in routine clinical practice. *Ann Clin Biochem.* 37(Pt3):253-61. https://doi.org/10.1258/0004563001899393
43. Prentoe J, Jensen TB, Meuleman P, et al. (2011) Hypervariable region 1 differentially impacts viability of hepatitis C virus strains of genotypes 1 to 6 and impairs virus neutralization. *J Virol.* 85(5):2224-34. https://doi.org/10.1128/jvi.01594-10
44. Mankowski MC, Kinchen VJ, Wasilewski LN, et al. (2018). Synergistic anti-HCV broadly neutralizing human monoclonal antibodies with independent mechanisms. *Proc Natl Acad Sci USA.* 115(1):E82-E91. https://doi.org/10.1073/pnas.1718441115
45. Mondelli MU, Cerino A, Boender P, et al. (1994). Significance of the immune response to a major, conformational B-cell epitope on the hepatitis C virus NS3 region defined by a human monoclonal antibody. *J Virol.* 68(8):4829-36. https://doi.org/10.1128/jvi.68.8.4829-4836.1994
46. Keck ZY, Xia J, Wang Y, Wang W, et al. (2012). Human monoclonal antibodies to a novel cluster of conformational epitopes on HCV E2 with resistance to neutralization escape in a genotype 2a isolate. *PLoS Pathog*. 8(4):e1002653. https://doi.org/10.1371/journal. ppat.1002653
47. Brasher NA, Adhikari A, Lloyd AR, et al. (2021). Hepatitis C Virus Epitope Immunodominance and B Cell Repertoire Diversity. *Viruses.* 13(6):983. https://doi.org/10.33 90%2Fv13060983
48. Liu J, Kong Y, Zhu L, et al. (2002). High-level expression of the C-terminal hydrophobic region of HCV E2 protein ectodomain in *E. coli*. *Virus Genes.* 25(1):5-13. https://doi.org/10.1023/a:1020136022896
49. Miroux B, Walker JE. (1996). Over-production of proteins in *Escherichia coli*: mutant hosts that allow synthesis of some membrane proteins and globular proteins at high levels. *J Mol Biol.* 19; 260(3):289-98. https://doi.org/10.1006/jmbi.1996.0399
50. Scheiblhofer S, Laimer J, Machado Y, et al. (2017). Influence of protein fold stability on immunogenicity and its implications for vaccine design. *Expert Rev Vaccines.* 16(5):479-489. https://doi.org/10.1080%2F14760584.2017.1306441
51. Popot JL. (1993). Integral membrane protein structure: transmembrane α-helices as autonomous folding domains: *Current opinion in structural biology* 3: 532–540. Curr Opin Struct Biol. 1993; 3(4):532–40. https://doi.org/10.1016%2F0959-440X(93)90079-Z
52. Dustin LB. (2017) Innate and Adaptive Immune Responses in Chronic HCV Infection. *Curr Drug Targets.* 18(7):826-843. https://doi.org/10.2174%2F1389450116666615082511 0532
53. Ströh LJ, Nagarathinam K, Krey T. (2018). Conformational Flexibility in the CD81-Binding Site of the Hepatitis C Virus Glycoprotein E2. *Front Immunol.* 9:1396. https://doi.org/10.3389/fimmu.2018.01396
54. Janeway CA Jr, Travers P, Walport M, et al. (2001). The Immune System in Health and Disease. 5th edition. New York: Garland Science; 2001. The major histocompatibility complex and its functions. *Immunobiology* https://www.ncbi.nlm.nih.gov/books/NBK27156/
55. Matzaraki V, Kumar V, Wijmenga C, et al. (2017). The MHC locus and genetic susceptibility to autoimmune and infectious diseases. *Genome Biol.* 18(1):76. https://doi.org/10.1186/s13059-017-1207-1.
56. Al Naqbi H, Mawart A, Alshamsi J, et al. (2021). Correction to: Major histocompatibility complex (MHC) associations with diseases in ethnic groups of the Arabian Peninsula. *Immunogenetics.* 73(2):153. https://doi.org/10.1007/s00251-021-01210-z
57. Li L, Petrovsky N, (2016). Molecular mechanisms for enhanced DNA vaccine immunogenicity. *Expert Rev Vaccines.* 15(3):313-29. https://doi.org/10.1586%2F14760584.2016.1124762
58. Sircy LM, Harrison-Chau M, Novis CL, et al. (2021). Protein Immunization Induces Memory $CD4^{+}$T Cells That Lack Th Lineage Commitment. *J Immunol.* 207(5):1388-1400. https://doi.org/10.4049/jimmunol.2100210
59. Zhu J, Yamane H, Paul WE, (2010). Differentiation of effector CD4 T cell populations. *Annu Rev Immunol.*28:445-89. https://doi.org/10.1146/annurev-immunol-030409-101212
60. Thimme R, (2021). T cell immunity to hepatitis C virus: Lessons for a prophylactic vaccine. *J Hepatol.* 74(1):220-229. https://doi.org/10.1016/j.jhep.2020.09.022